$$\mathbf{u} = \sum_{i=1}^{4} h_i \mathbf{u}_i + \sum_{i=1}^{4} \mathbf{H}_i^{en} \mathbf{u}_i^{en} \quad \text{with} \tag{3}$$

$$\mathbf{H}_i^{en} = h_i \begin{bmatrix} \xi_i & \eta_i & 0 & 0 \\ 0 & 0 & \xi_i & \eta_i \end{bmatrix}, \quad \mathbf{u}_i^{en} = \begin{bmatrix} u_i^{\xi} & u_i^{\eta} & v_i^{\xi} & v_i^{\eta} \end{bmatrix}^{\mathrm{T}},$$

where $\xi_i = (x - x_i)/\lambda_i$ and $\eta_i = (y - y_i)/\lambda_i$, in which λ_i is the largest diagonal length of element in cover i. Note that only the displacement field is enriched and the geometry interpolation of enriched finite element is identical to the standard finite element.

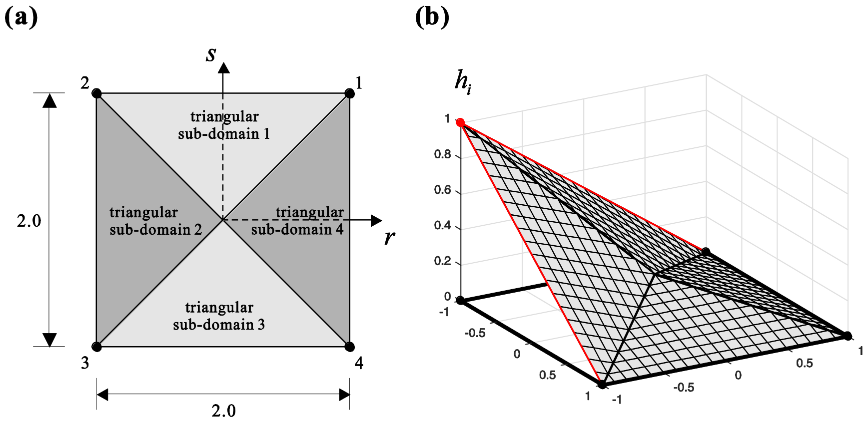

Fig. 2 Piecewise linear shape function: (a) triangular subdivision of quadrilateral element and (b) piecewise linear shape function corresponding to node i (Kim and Lee).

3. LINEAR DEPENDENCE PROBLEM

In this section, we investigate the linear dependence problem. The rank deficiencies of the global stiffness matrices are calculated by counting zero eigenvalues. Fig. 3 shows regular and distorted meshes are used to construct the global stiffness matrices, and the calculated rank deficiencies are presented in Table. 1.

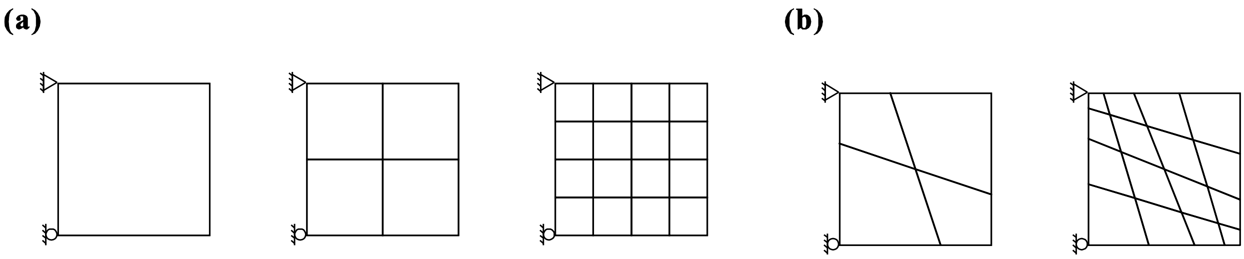

Fig. 3 Quadrilateral meshes: (a) square meshes and (b) distorted meshes (Kim and Lee).

As mentioned in the previous section, by applying the piecewise linear shape function, rank deficiency is not observed regardless mesh topology and enrichment function. Note that the $\mathbf{u}_i^{en}$ is suppressed at the fixed boundary, and this condition is applied in numerical examples in the next section.

Table 1. The rank deficiencies of the global stiffness matrices. Meshes shown in Fig. 3 are used.

Mesh type	Number of elements	Rank deficiency / Total degrees of freedom	
		Linear enrichment	Quadratic enrichment
Square	1	0/13	0/25
	4	0/43	0/85
	16	0/139	0/277
Distorted	4	0/43	0/85
	16	0/139	0/277

4. NUMERICAL EXAMPLES

In this section, we consider a wrench problem where the static analysis is performed and Cook's skew beam problem where the transient response is calculated.

4.1 WRENCH PROBLEM

The wrench problem shown in Fig. 4(a) is solved. Wrench is subjected to a uniform pressure load on line AA. We first perform the linear static analysis using 143 4-node standard finite elements, and then we selectively enrich nodes that are in high stress gradient area as shown in Fig. 4(b). The number of degrees of freedom in each case are 360 and 666. Calculated effective stress along line BB are presented in Fig. 5. By applying enrichment functions adaptively, the accuracy of solution is improved effectively.

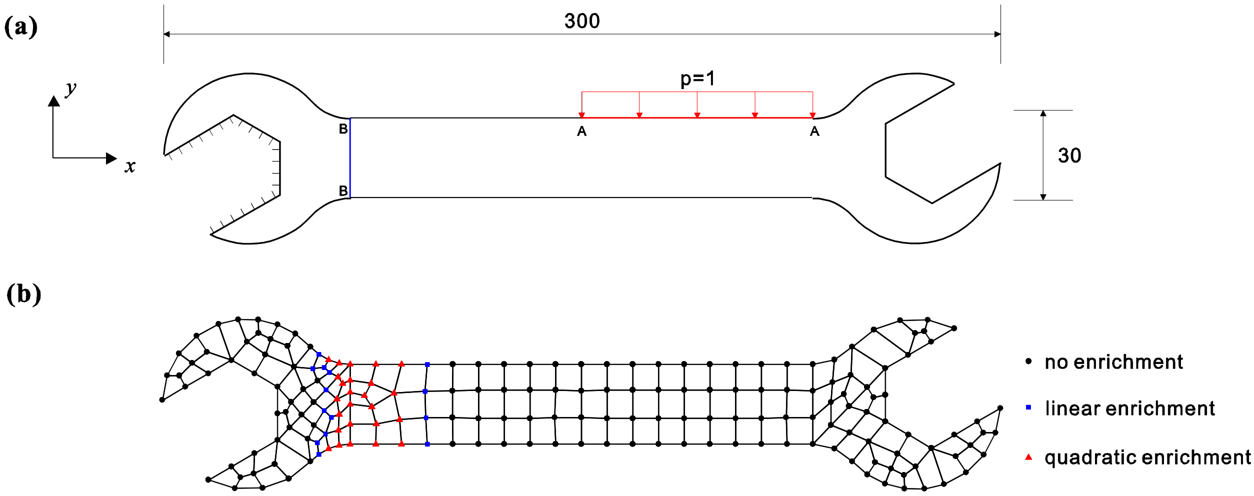

Fig. 4 Wrench problem: (a) problem description and (b) mesh used ($E = 1.0 \times 10^7$ and $\nu = 0.3$).

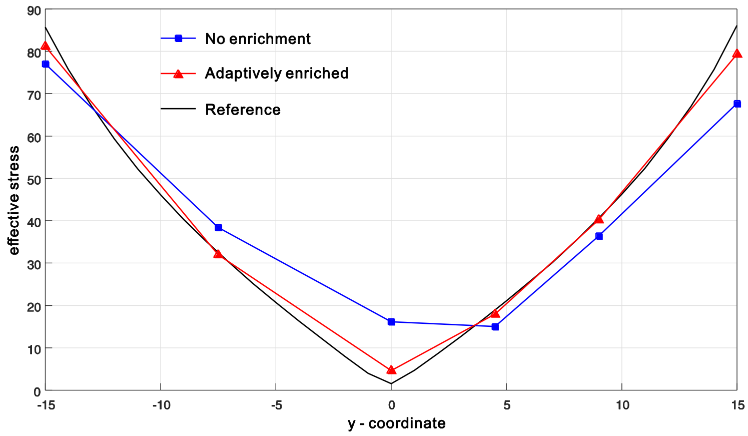

Fig. 5 Effective stress distribution along line BB shown in Fig. 4(a).

4.2 COOK'S SKEW BEAM PROBLEM

Transient response of the cook's skew beam shown in Fig. 6 is calculated. Newmark time integration method with time step $\Delta t = 0.001$ is used, and the initial condition is ${}^0\mathbf{U} = {}^0\dot{\mathbf{U}} = {}^0\ddot{\mathbf{U}} = \mathbf{0}$. We perform numerical simulations using

- 32x32 standard 4-node elements (2112 DOFs),
- 16x16 standard 9-node elements (2112 DOFs),
- 16x16 enriched 4-node elements with linear enrichment (1632 DOFs),
- 8x8 enriched 4-node elements with quadratic enrichment (864 DOFs),

and the results are presented in Fig. 7.

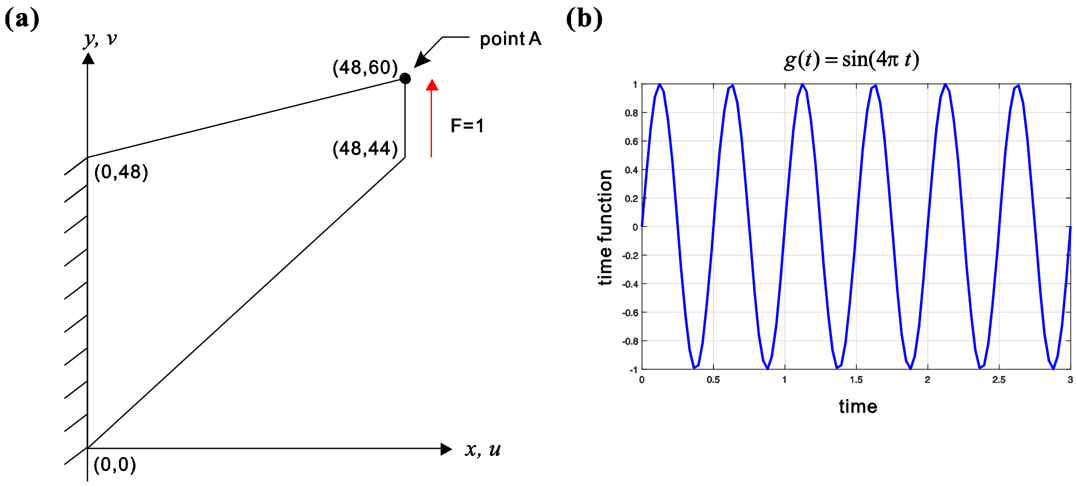

Fig. 6 Cook's skew beam problem: (a) problem description and (b) time function of applied load ($E = 1.0$, $\nu = 1/3$, and $\rho = 0.3\times10^{-4}$).

Except standard 4-node elements, results of the other elements are in good agreement with reference solution. The result shows that the new enriched 4-node finite element can provide more accurate solutions even with a smaller degree of freedoms than the standard finite elements.

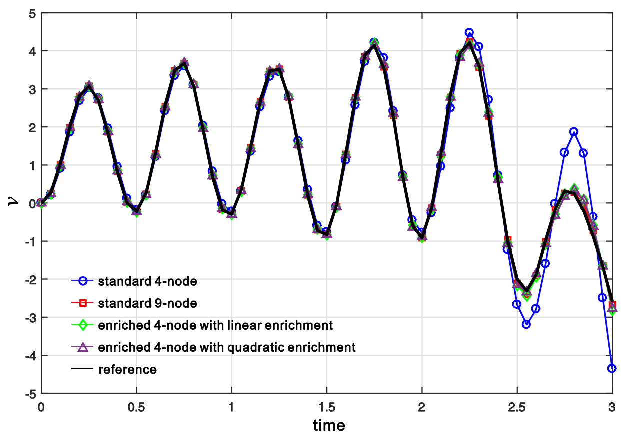

Fig. 7 Displacements response at point A shown in Fig. 6(a).

5. CONCLUSIONS

In this paper, a new enriched 4-node 2D solid finite element was introduced. The geometry and displacement interpolations of the new enriched 4-node 2D solid finite element are based on the piecewise linear shape function, and this element is free from the linear dependence problem. In the wrench problem, the effectiveness of the adaptive enrichment scheme was demonstrated, where the solution is improved without mesh refinement. Transient response of the cook's skew beam was also effectively obtained using enriched elements in terms of the number of degrees of freedoms. The development of enriched 3D solid finite elements and shell elements free from the linear dependence problem can be the future research (Lee and Bathe, 2004, Lee et al, 2012, Jeon et al, 2014, Lee et al, 2014, Jeon et al, 2015, Lee et al, 2015, Ko et al, 2017).

ACKNOWLEDGEMENTS

This work was supported by the Basic Science Research Program through the National Research Foundation of Korea (NRF) funded by the Ministry of Science, ICT & Future Planning (No. 2014R1A1A1A05007219), and the grant (MPSS-CG-2015-01) through the Disaster and Safety Management Institute funded by Ministry of Public Safety and Security of Korean government.

REFERENCES

An, X. M., Li, L. X., Ma, G. W., Zhang, H. H. (2011), “Prediction of rank deficiency in partition of unity-based methods with plane triangular or quadrilateral meshes”, *Computer Methods in Applied Mechanics and Engineering,* **200(5)***,* 665-674.

Bathe, K. J. (1996), “Finite element procedures”, *Prentice Hall*, New York.

Babuška I, Melenk JM. (1997), “The partition of unity method”, *International Journal for Numerical Methods in Engineering*, **40**, 727–58.

Dolbow, J. O. H. N., Belytschko, T. (1999), “A finite element method for crack growth without remeshing”, *International Journal for Numerical Methods in Engineering*, **46(1)**, 131-150.

Duarte, C. A., Babuška, I., Oden, J. T. (2000), “Generalized finite element methods for three-dimensional structural mechanics problems”, *Computer & Structures*, **77(2)**, 215-232.

Ham, S., Bathe, K. J. (2012), “A finite element method enriched for wave propagation problems”, *Computer & Structures*, **94**, 1-12.

Jeon, H.M., Lee, P.S., Bathe, K.J. (2014), “The MITC3 shell finite element enriched by interpolation covers”, *Computer & Structures*, **134**, 128-142.

Jeon, H. M., Lee, Y., Lee, P. S., Bathe, K. J. (2015), “The MITC3+ shell element in geometric nonlinear analysis”, *Computer & Structures*, **146**, 91-104.

Kim, J., Bathe, K.J. (2013), “The finite element method enriched by interpolation covers”, *Computer & Structures*, **116**, 35-49.

Kim, J., Bathe, K. J. (2014), “Towards a procedure to automatically improve finite element solutions by interpolation covers”, *Computer & Structures*, **131**, 81-97.

Kim, S., Lee, P.S., “Resolving the linear dependence problem of the 4-node 2D solid finite element enriched by interpolation covers”, *Computer & Structures*, submitted.

Ko, Y., Lee, P. S., Bathe, K. J. (2017), “A new MITC4+ shell element”, *Computer & Structures*, **182**, 404-418.

Lee, P. S., Bathe, K. J. (2004), "Development of MITC isotropic triangular shell finite elements", *Computer & Structures*, **82(11)**, 945-962.

Lee, Y., Yoon, K., Lee, P. S. (2012), "Improving the MITC3 shell finite element by using the Hellinger–Reissner principle", *Computer & Structures*, **110**, 93-106.

Lee, Y., Lee, P. S., Bathe, K. J. (2014), "The MITC3+ shell element and its performance", *Computer & Structures*, **138**, 12-23.

Lee, Y., Jeon, H. M., Lee, P. S., Bathe, K. J. (2015), "The modal behavior of the MITC3+ triangular shell element", *Computer & Structures*, **153**, 148-164.

Tian R, Yagawa G, Terasaka H. (2006), "Linear dependence problems of partition of unity-based generalized FEMs", *Computer Methods in Applied Mechanics and Engineering,* **195**, 4768–82.

Yoon, K., Lee, Y., Lee, P. S. (2012), "A continuum mechanics based 3-D beam finite element with warping displacements and its modeling capabilities", *Structural Engineering and Mechanics*, **43(4)**, 411-437.